Catalysis Science & Technology

Accepted Manuscript

This article can be cited before page numbers have been issued, to do this please use: O. Martin and J. Pérez-Ramírez, *Catal. Sci. Technol.*, 2013, DOI: 10.1039/C3CY00573A.

Dynamic Article Links ▶
View Article Online
DOI: 10.1039/C3CY00573A

Cite this: DOI: 10.1039/c0xx00000x

www.rsc.org/xxxxxx

ARTICLE TYPE

New (revisited) insights into the promotion of methanol synthesis catalysts by CO_2

Oliver Martin[a] and Javier Pérez-Ramírez*[a]

Received (in XXX, XXX) Xth XXXXXXXXX 20XX, Accepted Xth XXXXXXXXX 20XX
DOI: 10.1039/b000000x

CO hydrogenation, CO_2 hydrogenation, and water-gas shift (WGS) reactions have been simultaneously investigated over industrial-like catalysts based on Cu-ZnO-Al_2O_3 under methanol synthesis conditions (513 K, 5.0 MPa). For this, a novel methodology has been applied: the concentration of carbon dioxide in the syngas feed was consecutively increased (R = CO_2:(CO+CO_2) = 0–100) resulting in a volcano-type plot of the rate of methanol formation and forming a hysteresis loop when decreasing the CO_2 concentration again. H_2O co-feeding experiments revealed that the enhancement of activity can be correlated with the WGS activity linking both hydrogenation paths of CO and CO_2. On the other hand, excessive amounts of surface hydroxyls seem to inhibit methanol production explaining the drop in activity at high CO_2 concentrations. The investigation of the catalytic performance was accompanied by an extensive characterisation of the fresh and used catalytic materials by X-ray diffraction, temperature-programmed reduction by H_2, N_2O pulse chemisorption, X-ray photoelectron spectroscopy, and Auger electron spectroscopy. It was unveiled that the copper surface area affects the CO_2 hydrogenation; however, this parameter is unambiguously not the key descriptor for CO_2-promoted methanol synthesis, which is a consequence of the synergistic interaction of zinc oxide and copper. This structural feature is further promoted by Al_2O_3 through stabilization of the surface. The position of the activity maximum is determined by the surface ratio Cu:Zn. The hysteresis behaviour is a result of the continuous decrease of Cu dispersion and the fixation of copper species in its monovalent oxidation state, both detrimental for CO_2 hydrogenation. CO hydrogenation is strongly affected by the Cu:Zn bulk ratio and thus the reducibility of the catalyst. These facts could be substantiated by the use of impregnated model catalysts.

1. Introduction

Methanol (MeOH) belongs to the top ten petrochemicals in the world.[1,2] It is further seen as a promising bridging technology for replacing fuels or serving as a chemical feedstock besides oil since syngas, which is needed for the production of methanol, can be obtained from different sources, *e.g.* coal or biomass.[3] Additionally, methanol synthesis offers currently the only possibility of utilising CO_2 emissions on large scale.[4] In the standard industrial process, a combined feed of CO, H_2, and CO_2 is converted into methanol over Cu-ZnO-Al_2O_3 catalysts (Cu:Zn:Al ~ 6:3:1) at temperatures of 493–573 K and total pressures of 5–10 MPa offering a selectivity higher than 99.9%.[1] Accordingly, the equilibria (eqn. (1–3)), *i.e.* CO and CO_2 hydrogenation and water-gas shift (WGS), are required for describing the methanol synthesis.[5]

The most relevant limitation in the commercial process is the thermodynamic one and thus high concentrations of CO_2 push the equilibrium towards an unfavourable regime.[6] However, operating at pure CO conditions does not result in high methanol yields due to kinetic reasons.[7] A certain amount of CO_2 (commonly (H_2−CO_2):(CO+CO_2) ~ 2) is crucial in the feed in order to reach a reasonable conversion.[8] The promotional effect by carbon dioxide has been demonstrated in several studies and has been speculatively assigned to the WGS reaction linking both hydrogenation routes.[7-9] Strong adsorption of reactants,[8,10,11] inhibition of CO hydrogenation by CO_2,[12] or the dependence on the oxygen coverage[13] have been controversially discussed in literature as reason for the drop in activity at high CO_2 concentrations. The investigations of relationships between the structural (surface) properties of the catalyst and the CO_2 promotion are even more speculative.

$$CO+2H_2 \leftrightarrows CH_3OH \qquad \Delta_R H_{493\,K} = -97.4\ kJ\ mol^{-1} \qquad (1)$$

$$CO_2+3H_2 \leftrightarrows CH_3OH+H_2O \qquad \Delta_R H_{493\,K} = -57.4\ kJ\ mol^{-1} \qquad (2)$$

$$CO+H_2O \leftrightarrows CO_2+H_2 \qquad \Delta_R H_{493\,K} = -40.0\ kJ\ mol^{-1} \qquad (3)$$

Extensive studies have been conducted in methanol synthesis tackling primarily how to obtain catalysts with high Cu surface area and how to stabilise such surfaces preventing sintering of the

[a] *Institute for Chemical and Bioengineering, Department of Chemistry and Applied Biosciences, ETH Zurich, Wolfgang-Pauli-Strasse 10, CH-8093 Zurich, Switzerland. Fax: +41 44 633 14 05; E-mail: jpr@chem.ethz.ch*

View Article Online
DOI: 10.1039/C3CY00573A

copper nanoparticles,[14] the main reason for deactivation.[1,2,15-17] In contrast, the research aiming at understanding the Cu-ZnO-Al_2O_3 catalyst remains highly contentious due to material and pressure gaps usually existing in those studies: model catalysts have been mostly used and the reaction has been operated at pressure conditions far below 5 MPa. Overcoming both deficiencies is crucial since the Cu-ZnO-Al_2O_3 system changes dynamically in structure depending on the process conditions, especially on the syngas composition.[15,18-20] This fact entails that static kinetic models are not sufficiently characterising the nature of the methanol synthesis mechanism.[21] Monitoring these alterations becomes consequently essential since it was proven for industrial-like catalysts that methanol synthesis is sensitive towards different facets of copper.[22] This valuable result was supported by density functional theory calculations within the same study revealing in addition that Cu surfaces, decorated by Zn atoms, offer reaction pathways of lower energy for both CO and CO_2 hydrogenation (*vide* Liu and co-workers[23]). The role of ZnO in the CO_2 promotion effect has not been unravelled in this work, nevertheless.

Klier *et al.*[8] investigated in 1982, for the first time, CO_2-promoted methanol synthesis over a Cu-ZnO catalyst by consecutively changing the concentration of carbon dioxide in the syngas feed from $R = CO_2:CO_x = 0$ to 100 ($CO_x = CO+CO_2$), which evidenced a huge increase of carbon oxide conversion for low contents of CO_2 compared to pure feeds of CO/H_2 or CO_2/H_2, respectively. This approach, following the catalyst history depending on R, has never again been seized extensively except in a few kinetic modelling studies.[12,13,24-27] However, none of these studies attempted to correlate the catalytic performance with the structure of the catalyst or went beyond the speculations by Klier *et al.*[8] who claimed the ratio R determines the redox properties of the copper surface.

We have found that this experimental approach discloses worthwhile insights when altering the composition of the catalyst and subsequently conducting complementary changes of R, resulting in a reversible hysteresis phenomenon. It consequently offers the possibility to tackle the complexity of the methanol synthesis process, *i.e.* three interconnected equilibria proceeding over the ternary catalyst Cu-ZnO-Al_2O_3. H_2O co-feeding experiments revealed the mechanistic nature of CO_2-promoted methanol synthesis. From the application of binary catalyst compositions (*i.e.* Cu-ZnO, Cu-Al_2O_3, and ZnO-Al_2O_3) we could gain valuable structure-performance relationships: ZnO is not solely a good disperser of copper nanoparticles, but it is required in Cu-based catalysts in order to observe the promotional effect by CO_2. This synergistic interaction of Cu and ZnO has been further investigated by varying the Cu:Zn ratio and by applying impregnated model catalysts.

2. Materials and Methods

2.1. Catalyst preparation

All catalysts have been synthesised either *via* co-precipitation, the standard industrial approach of preparing methanol synthesis catalysts,[1] or impregnation. Co-precipitation was conducted by mixing two 1 M solutions containing either Na_2CO_3 (Acros Organics, 99.8%) or the corresponding mixture of metal nitrates, $Cu(NO_3)_2{\cdot}3\ H_2O$ (Sigma-Aldrich, 98%), $Zn(NO_3)_2{\cdot}6\ H_2O$ (Acros Organics, 98%) and/or $Al(NO_3)_3{\cdot}9\ H_2O$ (Alfa Aesar, 98%), in the desired molar ratio reaching a final pH 8.0 of the slurry. The precipitates were directly filtered without ageing and subsequently the filter cake was washed by deionised H_2O until pH 7.0 was reached in the filtrate. Finally, it was dried at 338 K overnight. Ternary and binary catalyst compositions, *i.e.* Cu-ZnO-Al_2O_3 and accordingly Cu-ZnO, Cu-Al_2O_3, ZnO-Al_2O_3, have been synthesised corresponding to this method and are denoted expressing their metal composition, *e.g.* CuZnAl for Cu-ZnO-Al_2O_3. Suffix figures refer to the molar ratio of Cu and Zn in the bulk, *e.g.* CuZn-2 for Cu-ZnO with ratio Cu:Zn = 2.

For impregnation, neutral γ-Al_2O_3 (MP Biomedicals, 99%) was dispersed in deionised water together with the metal precursors, $Cu(CH_3COO)_2{\cdot}H_2O$ and/or $Zn(CH_3COO)_2{\cdot}2\ H_2O$ (both from Sigma-Aldrich, 99%). The stirred slurry was fed to a Büchi mini spray dryer B-290 applying a liquid flow rate of 5.3 cm^3 STP min^{-1}, a flow rate of spraying air of 450 cm^3 STP min^{-1} and a flow rate of heated air stream of 0.6 m^3 STP min^{-1} and heating the inlet to 493 K. All as-synthesised materials were finally calcined at 573 K for 2 h in static air, ramping by 2 K min^{-1}.

2.2. Characterisation

All catalysts were characterised by powder X-ray diffraction (XRD) at any stage of the preparation, *i.e.* as-synthesised, calcined, reduced, and after the catalytic test, on an X'Pert Pro MPD from PANalytical utilising Cu-K_α radiation (λ = 0.1542 nm) with an angular step size of 0.033° 2θ and a counting time of 8 s per step. Particle sizes of reduced copper were estimated from Cu(1 1 1) reflection using the Scherrer equation. No other crystalline phases than Cu metallic or ZnO were detected by XRD after reduction or reaction. N_2 isotherms were obtained at 77 K on a Quadrasorb SI Quantachrome instrument, calculating the total surface area by BET method. Samples were degassed before the measurement by heating them up to 473 K in vacuum for 3 h.

The metal content (Cu, Zn, and Al) of the calcined samples was determined by ICP-OES (inductively coupled plasma – optical emission spectroscopy) on a Horiba Ultima2 applying an Ar plasma. Each sample was previously heated to 373 K in a mixture of aqua regia and HF (volumetric ratio = 1:6) for completely dissolving the catalysts. Both, temperature-programmed reduction by H_2 (H_2-TPR) and N_2O pulse chemisorption, were run on a Thermo TPDRO 1100 set-up equipped with a TCD (thermal conductivity detector). Prior to analysis, the catalysts were dried in He at 373 K for 30 min. Subsequently, the H_2-TPR experiments were conducted ramping from 323 to 673 K by 2 K min^{-1} in 5 mol-% H_2 in N_2 at atmospheric pressure. The copper surface area was identified by pulsing N_2O at 363 K over the catalyst that was dried and reduced under H_2-TPR conditions (*vide supra*), however, levelling the temperature off at 503 K for 2 h.[28]

X-ray photoelectron spectroscopy (XPS) and Auger electron spectroscopy (AES) were performed on a VG-Microtech Multilab 3000 spectrometer featuring a hemispheric electron analyser with 9 channeltrons and non-monochromatised Mg-K_α radiation at 1253.6 eV. The used catalyst was cooled down to room temperature under nitrogen atmosphere before transferring the

View Article Online
DOI: 10.1039/C3CY00573A

sample under ultra-high vacuum conditions (residual pressure of ca. 5 10^{-7} Pa) into the analysis chamber of the spectrometer. The spectra were collected at a pass energy of 50 eV. The intensities were estimated by calculating the integral peak, after subtracting the S-shaped background, and by fitting the experimental curve to a linear combination of Lorentzian and Gaussian functions scaled by a ratio of 30:70. The binding energy scale was referenced to the C 1s level of the carbon overlayer at 284.6 eV. 933.6 eV and 932.1 eV have been used as binding energies to distinguish Cu^{2+} and Cu^{red}, the latter species combines copper in reduced state, *i.e.* Cu^+ and Cu^0, which cannot be distinct on the basis of XPS.[29]

2.3. Catalytic evaluation

A home-made fixed-bed reactor set-up was built tackling industrial methanol synthesis conditions, *i.e.* $T \leq 573$ K, $P \leq 10.0$ MPa. For liquid injection, an HPLC (high-performance liquid chromatography) pump 307 (Gilson) was connected to the heated part on top of the reactor. All gases were obtained from Pangas/Linde with a purity ≥99.99995%. Online analysis of the outlet gas stream was carried out by gas chromatography (GC, Agilent 7890A), using a GS-CARBONPLOT column for separating CO, CO_2, N_2, and H_2 coupled to a TCD and a DB-1 column to analyse all organic compounds by a flame ionisation detector (FID).

Methanol synthesis could potentially form hotspots in the catalyst bed due to its elevated exothermic nature. However, we have not diluted the bed since Villa *et al.*[30] have calculated the external heat transfer to be as low as ~1 K. It was anticipated that the internal heat transfer is even lower for the small particles applied (125–300 µm sieved fraction) corroborated by the fact that no difference between the temperature of the oven and the bed could be determined. The activation of the catalysts was done *in situ* and consisted of a drying step at 433 K (2 K min^{-1}) for 30 min in a flow of N_2 and of a reduction step at 503 K (2 K min^{-1}) for 2 h in 5 mol-% H_2 in N_2 at 0.5 MPa total pressure, referred to as fresh sample. Finally, desired reaction conditions were applied; typically 513 K, 5.0 MPa total pressure, H_2:CO_x = 7, WHSV = 7.5 h^{-1}. These conditions were used to ensure working below thermodynamic limitation. N_2 was used as internal standard at a fixed mole fraction of $x(N_2) = 0.28$. Water-gas shift activity was conducted at same conditions feeding a gas stream of $x(CO) = 0.09$, H_2O:CO = 1–5, GHSV = 16,000 h^{-1}, N_2-balanced. After each reaction, the catalyst was passivated by flushing with 2 mol-% O_2 in N_2 at 323 K for 1 h.

Carbon balance was determined for each experiment to be less than 5% in deviation. All co-precipitated catalysts performed with a selectivity of methanol >99% in terms of organic products. The only by-product, which was formed in the case of the spray-dried catalysts, was determined to be dimethyl ether (DME). The relative uncertainty of the formation rate of MeOH and DME has been estimated from an error propagation calculation to be 6% on average. All catalytic tests were reproduced within error range.

3. Results and discussion

3.1. The source of CO_2 promoted methanol synthesis

The basic characterisation of the catalysts utilised in this study is given in Table 1. CO_2 promotion was initially studied over conventionally co-precipitated, ternary Cu-ZnO-Al_2O_3, denoted as CuZnAl (Fig. 1). The parameter $R = CO_2$:CO_x expresses the CO_2 concentration in the syngas feed. The experiment is named CO or CO_2 cycle when starting the alteration of R from 0 or 100, respectively. For a clear assignment, the branch to be referred to at

Table 1 Catalytic materials that have been synthesised und tested within this study.

Denotation	Method	S_{Cu} [d] / m^2 g^{-1}	Molar Cu:Zn:Al[e]
CuZnAl or CP	[a]	15.6±0.5	6.0:2.8:1.4
CuZn or CuZn-2	[a]	13.7±0.4	6.0:2.4:0
CuZn-0.5	[a]	3.8±0.1	6.0:12.4:0
CuZn-10	[a]	5.8±0.2	6.0:0.6:0
CuAl	[a]	5.4±0.2	6.0:0:1.4
ZnAl	[a]	–	0:3.0:1.5
SD	[b]	2.2±0.1	6.0:3.1:163
Cu@Zn	[c]	1.1±0.1	3.0:6.1:187

[a] Co-precipitation. [b] Simultaneously spray-dried $Cu(CH_3COO)_2$ and $Zn(CH_3COO)_2$ on Al_2O_3. [c] $Cu(CH_3COO)_2$ spray-dried on ZnO/Al_2O_3. [d] Determined by N_2O pulse chemisorption on the fresh catalysts. [e] ICP-OES.

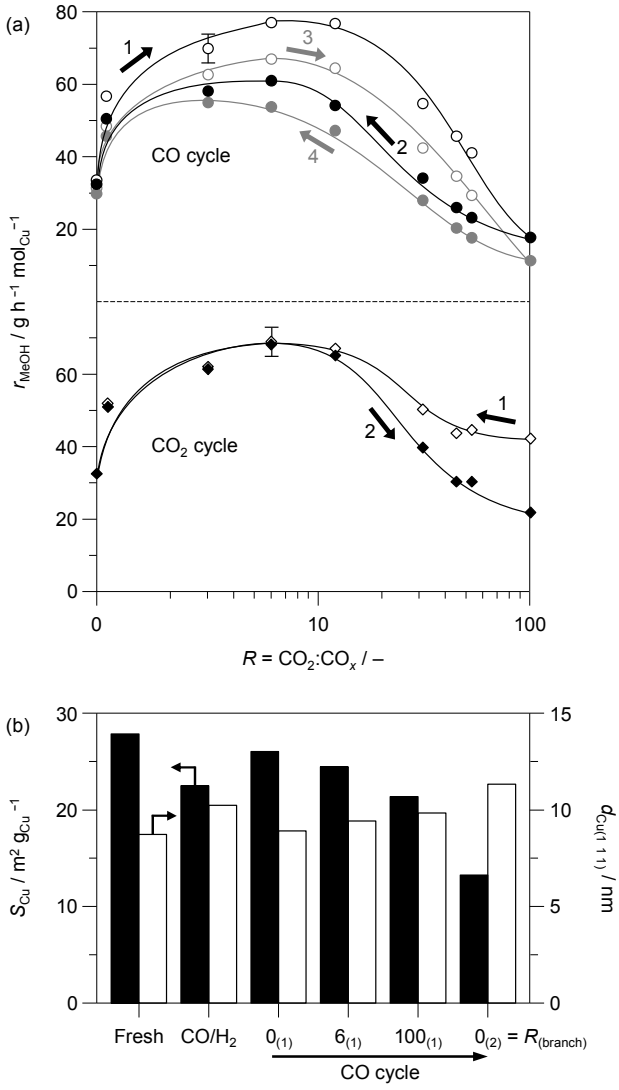

Fig. 1 (a) Rate of methanol formation per mol of exposed Cu (r_{MeOH}) over CuZnAl at 513 K, 5.0 MPa, and H_2:CO_x = 7: consecutively changing the

View Article Online
DOI: 10.1039/C3CY00573A

CO_2 concentration starting from $R = 0$ (circles, CO cycle) or $R = 100$ (diamonds, CO_2 cycle). Branch 3 and 4 (top) refer to a second subsequent CO cycle. (b) Corresponding evolution of copper surface areas (S_{Cu}, black bars) and particle sizes of Cu(1 1 1) facet ($d_{Cu(1\,1\,1)}$, white bars) along the CO cycle. Additionally, the characterisation of the sample is shown which has been operated at $R = 0$ (CO/H_2) maintaining the same time-on-stream that was necessary to run one CO cycle (~60 h).

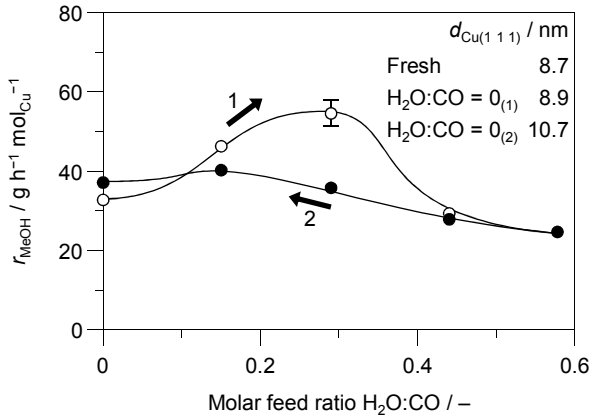

Fig. 2 H_2O cycle over CuZnAl at 513 K, 5.0 MPa, $H_2:CO = 7$: water steam has been co-fed to the syngas and the $H_2O:CO$ ratio was consecutively altered. Copper particle sizes are given for the fresh catalyst and the catalyst before and after H_2O co-feeding.

a particular value of R is given additionally in brackets as subscript.

The observations that CO_2 hydrogenation is favoured over CO hydrogenation (compare $R = 0_{(1)}$ and $100_{(1)}$ of CO and CO_2 cycle, respectively, in Fig. 1a) and that a maximum of methanol production occurs by increasing or decreasing R coincide with the results from literature.[7,8,13,31] A novel result is the presence of a hysteresis when the CO_2 concentration is decreased again in the CO cycle. Methanol synthesis catalysts are thus highly affected by their history.[20] This sensitivity was exploited to gather performance-mechanism-structure relationships.

It is thus necessary to discuss the former dogma that copper surface area is the key parameter of methanol synthesis catalysts[17] taking the several studies into account, which indicated other aspects being relevant such as Cu-ZnO interactions.[32-35] First of all, CO hydrogenation and CO_2 hydrogenation must be clearly distinct since MeOH production from CO_2 depends on the catalyst history whereas CO hydrogenation obviously does not within the cycle experiment. Copper surface area and particle size according to the Cu(1 1 1) facet show the continuous decrease or increase, respectively, monitored over the CO cycle (Fig. 1b). CO hydrogenation ($R = 0$) results always in the same reaction rate independent of Cu dispersion. In contrast, CO_2 hydrogenation ($R = 100$) exhibits only half of the initial rate when starting from CO or at the end of the CO_2 cycle. It appears to be therefore sensitive to the Cu dispersion.

The effect of CO_2 promotion cannot be correlated with the dispersion of copper which follows a different trend than the methanol production does along R. The enhancement of activity must be therefore the consequence of (i) either the formation of special catalytically active sites at particular syngas compositions and/or (ii) the beneficial involvement of the WGS reaction. The latter aspect has been tested by starting the reaction at $R = 0$ and consecutively varying the concentration of co-fed H_2O steam (Fig. 2), referred to as H_2O cycle, akin to the CO cycle (Fig. 1a). A promotional effect and a hysteresis were observed, too. This result corroborates the hypothesis that WGS is mechanistically the source of CO_2 promotion by converting carbon monoxide into CO_2, which is supposed to be the main source in methanol synthesis.[7,13,36] H_2O plays consequently an ambivalent role as CO_2 in methanol synthesis: promotional when small concentrations are

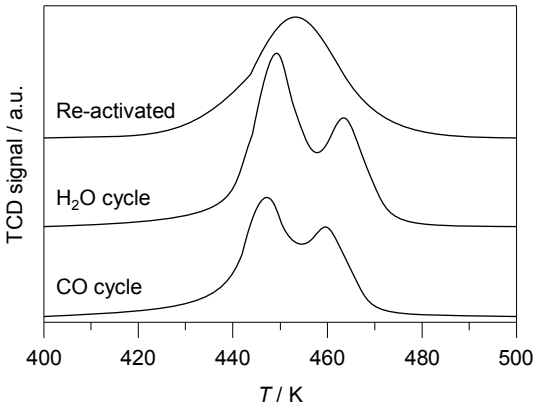

Fig. 3 H_2-TPR profiles of CuZnAl recorded after one CO cycle (*vide* Fig. 1a, top) and after the H_2O cycle (*vide* Fig. 2). Re-activated refers to the sample used in the following sequence: CO cycle → re-activation → CO cycle (*vide* Fig. 4a).

present and deactivating by excessive co-feeding.[37]

One reason for the deactivation at high concentrations of H_2O or CO_2 is probably that the increased coverage by hydroxyl species inhibits the CO_2 hydrogenation (*vide* Fig. SI1), *e.g.* through blocking of active sites.[13,38,39] A second point is the irreversible loss of Cu surface area leading to an increased Cu particle size. The sintering is amplified when H_2O is introduced in the feed (Fig. 2). This substantiates the conclusion that CO_2 hydrogenation is sensitive towards Cu dispersion. Apesteguía *et al.*[40] have shown that also the WGS itself is enhanced by increased dispersion of copper. This would in turn be one explanation for the hysteresis behaviour.

The fact that a higher molar ratio of $H_2O:CO = 0.3$ is necessary for reaching the maximum activity, compared to $CO_2:CO = 0.06$ in the dry cycle, relies most probably on CO_2 being a molecule that itself is quickly converted into methanol. Additionally, the standard reduction potential of H_2O is much more negative than the one of CO_2[31] and thus the strength of their influence on the catalyst surface will differ, too; however, the reducible surface sites of the catalyst are the same after both experiments according to the H_2-TPR profiles (Fig. 3).

The correlation of WGS activity and CO_2 promotion is unequivocally demonstrated by Fig. 4: CuZnAl was re-calcined (2 mol-% O_2 in N_2, 0.5 MPa, 573 K, 2 K min^{-1}, 2 h) and re-reduced before conducting WGS reaction or a second CO cycle, respectively. Both MeOH synthesis performance (Fig. 4a) and WGS activity (Fig. 4b) are significantly lowered after re-activating the catalyst. This is most likely to be caused by morphological changes since 90% of copper surface area is lost

View Article Online
DOI: 10.1039/C3CY00573A

compared to the fresh catalyst. Water-gas shift must be therefore seen as an essential step in CO_2-promoted methanol synthesis rather than being a side reaction.

3.2. Evolution of copper surface upon reaction

The presence of hysteresis in the CO cycle revealed that the deactivation effects cannot be solely a result of the mechanism, *i.e.* the interplay between CO_2 promotion and hydroxyl coverage. It is also unlikely that the behaviour can be generally explained by a non-steady state of the catalyst since the hysteresis is preserved in the second CO cycle (Fig. 1a). It turned out that these effects have

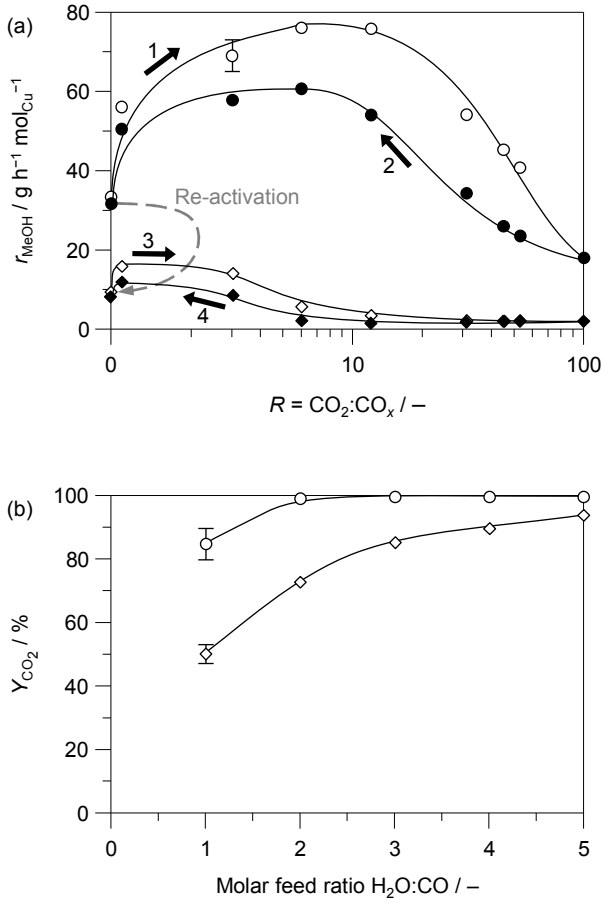

Fig. 4 (a) CO cycle profiles (conditions as before) and (b) water-gas shift activity at 513 K, 5.0 MPa, H_2O:CO = 1−5 in terms of yield of carbon dioxide (Y_{CO2}) over fresh CuZnAl (circles) and CuZnAl that was operated for one CO cycle and subsequently re-activated (diamonds), *i.e.* re-calcined and re-reduced.

to be correlated with the composition of the catalyst surface. This is indicated by the H_2-TPR profiles recorded after the experiments (Fig. 3): the bimodal profile is the same after conducting the CO or the H_2O co-feeding cycle, but it is significantly changed for re-activated CuZnAl. This alludes to the assumption that the morphology[41-43] and/or the redox properties of surface Cu/ZnO_x are significantly altered over re-activation.

In order to unveil the influence of the syngas composition on the catalyst surface, XPS and AES have been carried out (Fig. 5). The Cu species clearly respond to the syngas composition as also stated by other authors:[8,29,44] prolonged exposition of the catalyst to CO/H_2 converts all copper surface species into Cu metallic. CO_2 hydrogenation conditions induce the formation of (partially) oxidised copper, Cu^+ and Cu^{2+}. Monovalent copper is also the major species at the maximum of CO_2 promotion (R = 6).

Interestingly, not all of the Cu^+ species can be re-converted to metallic copper anymore as soon as the catalyst has been treated by CO_2 hydrogenation conditions; clearly demonstrated by AES of the catalyst after the CO cycle (Fig. 5b, $R = 0_{(2)}$). This finding gives an explanation for the hysteresis behaviour in addition to the drop of Cu surface area. The slight enhancement of Cu^0 after the cycle likely stems from the reduction of Cu^{2+} which was formed along the cycle. The partially re-reduced Cu surface after the first cycle

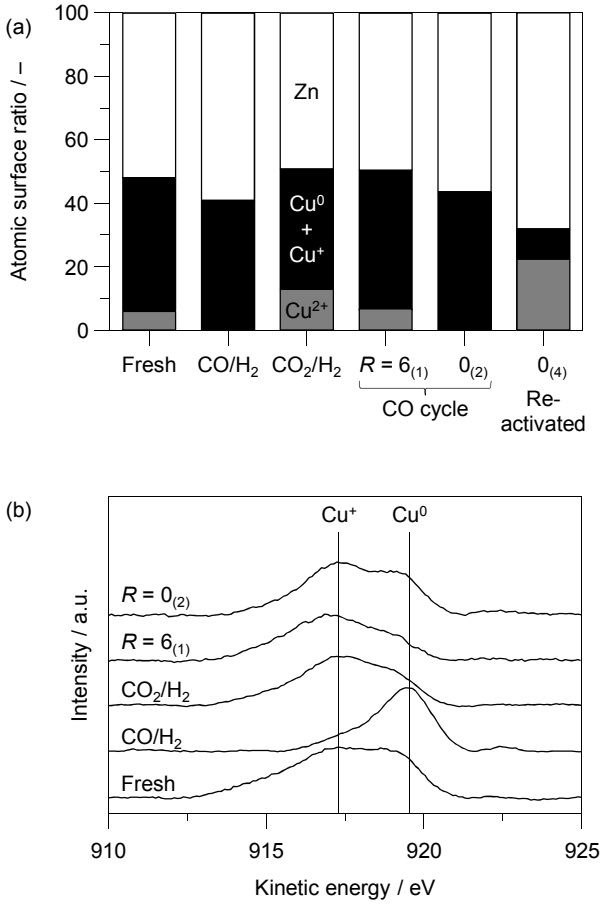

Fig. 5 Monitoring of the surface changes of CuZnAl upon the CO cycle (*vide* Fig. 4a) by XPS and AES: (a) surface composition regarding Zn, Cu^0/Cu^+, and Cu^{2+}, estimated from the deconvolution of the XPS spectra; (b) corresponding Auger Cu LMM spectra. Both figures include the data of the catalyst exposed to fixed syngas conditions (CO/H_2 or CO_2/H_2, respectively).

could then be the reason why branch 3 (second cycle) exceeds branch 2 (first cycle).

The issue has been controversially debated for decades which copper site is the active one in methanol synthesis. Monnier *et al.*[45] found a linear correlation of the amount of Cu^+ in Cu-Cr_2O_3 catalysts and their activity for CO hydrogenation. They demonstrated subsequently that this type of catalyst does not exhibit a promotional effect by CO_2 at 543 K and 5.2 MPa like ZnO-containing catalysts.[46] They concluded that ZnO and Cr_2O_3

View Article Online
DOI: 10.1039/C3CY00573A

possess a different ability to stabilise Cu^+ species under reaction conditions: Cr_2O_3 locks the oxidation state of copper whereas ZnO allows dynamic alteration of it.

CO_2 hydrogenation proceeds over similar surface compositions with different activities (compare Table SI1, entry 4 and 8). It is therefore questionable whether Cu^+ is an active site for this reaction. Especially the required scission of the C-O bond might occur preferentially on Cu metallic. In contrast, CO hydrogenation results in a similar performance irrespective of the alteration of the surface. We conclude from this result that CO is converted to methanol over both Cu^0 and Cu^+, but monovalent copper has no promotional effect on the CO hydrogenation itself. Monovalent copper species might consequently only account for the WGS

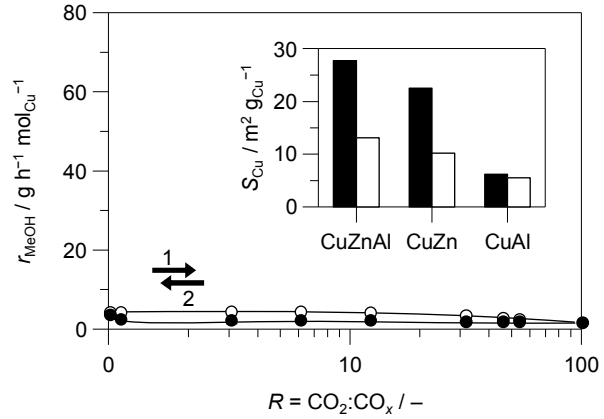

Fig. 6 CO cycle over binary CuAl (conditions as before). The corresponding ZnAl possesses only poor activity of approximately 0.1% conversion of CO_x without indication of hysteresis behaviour. Inset: copper surface areas of the ternary and the binary co-precipitated catalysts fresh (black) and after one CO cycle (white).

reaction in the CO_2 promotion.

XPS also disclosed that re-activating CuZnAl results in a catalyst surface with a high fraction (~75%) of inactive Cu^{2+} (Fig. 5a). The fact that this Cu species cannot be converted into (partially) reduced ones, despite of the strong reducing conditions at $R = 0$, shows that morphological changes most likely occurred, which also influenced the stabilisation of Cu in its different oxidation states.

3.3. Impact of metal oxides on CO_2 promotion

The monitored dynamics of copper oxidation states lead to the assumption that a strong interaction with the metal oxides, ZnO and Al_2O_3, is present in methanol synthesis catalysts and is supposed to dictate the performance. This is unveiled on the basis of extending the cycle approach towards binary catalyst compositions, particularly Cu-ZnO (CuZn), Cu-Al_2O_3 (CuAl), and ZnO-Al_2O_3 (ZnAl). The low activity of CuAl (Fig. 6) and the inactivity of ZnAl coincide with reported results.[2] CO_2 promotion is only observed for the Cu-ZnO catalyst and is a consequence of strong synergism between Cu and ZnO (Fig. 7). This is a clear evidence of ZnO being an essential partner in CO_2-promoted methanol synthesis. The unique collaboration of Cu and ZnO was already observed by other authors[18,47,48] and has been controversially discussed.[17] However, we could demonstrate that the Cu-ZnO synergy is necessary in order to observe the promotional effect. Obviously, this structural interaction reveals the key for understanding methanol synthesis catalysts.

Table 2 Evolution of catalysts properties as a function of Cu:Zn bulk ratio.

Cu:Zn[a]	$S_{Cu,rel}$[b,c] / %	$S_{ZnO,rel}$[d] / %	S_{Cu}[b] / m^2 g$_{Cu}^{-1}$ Fresh	After cycle
0.5	15	85	16.0±0.5	5.9±0.2
2	36	64	22.5±0.7	10.2±0.3
10	38	62	6.6±0.2	1.6±0.1

[a] Determined by ICP-OES on the basis of the calcined materials. [b] Analysed by N_2O pulse chemisorption on the fresh catalyst. [c] Surface ratios are referred to the BET N_2 surface area as total area of the fresh catalyst. [d] Estimated from the difference of BET N_2 surface area and S_{Cu}; this approach is reliable since ZnO does not chemisorb oxygen irreversibly from N_2O.[15]

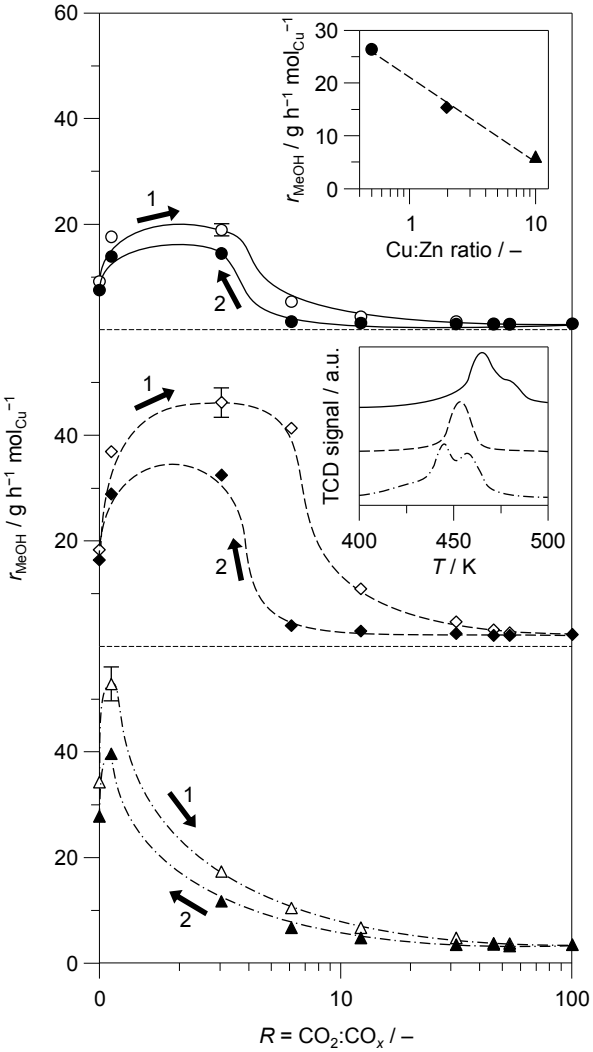

Fig. 7 CO cycle (conditions as before) of CuZn catalysts of different Cu:Zn ratios = 0.5 (–·–), 2 (□ □), and 10 (—). Insets: (top) CO hydrogenation activity at $R = 0_{(2)}$ as a function of Cu:Zn ratio; (middle) respective H_2-TPR profiles (signals normalised on catalyst mass).

Contradictory, Chinchen *et al.*[49] concluded that the CuZnAl catalyst is solely the sum of its components. Indeed, this is true in terms of copper surface area (Fig. 6, inset): both metal oxides are necessary to highly disperse copper nanoparticles. However, it

View Article Online
DOI: 10.1039/C3CY00573A

has been observed that a physical mixture of Cu/SiO_2 and ZnO/SiO_2 is much more active than the sum of both single components utilising $CO/CO_2/H_2$ mixtures, respectively.[50] This fact and the absence of CO_2 promotion over CuAl elucidate that there is a synergistic effect between Cu and ZnO, which has been a matter of hot debate in literature.

It could be thus anticipated that the Cu:Zn ratio will influence the performance of the catalyst. The position of the maximum could be correlated with the Cu:Zn surface ratio: the higher the bulk ratio, the greater the surface concentration of Cu (Table 2), and the more the maximum is shifted towards greater R (Fig. 7); in line with the higher Cu:Zn surface ratio of the ternary catalyst (Fig. 5a) and its maximum at higher CO_2 concentration (Fig. 1a). The amount of Cu on the catalyst surface is levelled off at a ratio of Cu:Zn ~ 40:60, comparing the samples Cu:Zn = 2 and 10 (Table

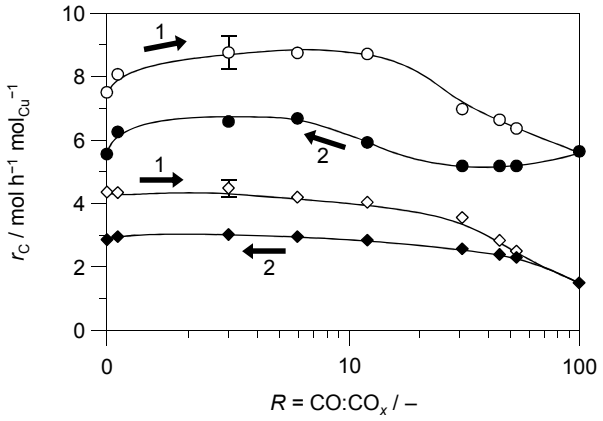

Fig. 8 CO cycle performance (conditions as before) over spray-dried catalysts as carbon-based product formation: (i) simultaneously deposited Cu and Zn precursor on Al_2O_3, Cu:Zn = 2 (SD, diamonds) and (ii) Cu precursor impregnated on ZnO/Al_2O_3, Cu:Zn = 0.5 (Cu@Zn, circles).

2). ZnO seems to exhibit a strong affinity to accumulate at the surface. This surface ZnO is very likely to influence the stabilisation of copper species in their different oxidation state. We consequently deduce that the dynamics in Cu^+ formation is a measure for the interaction of Cu and ZnO.

Besides, the alteration in Cu:Zn bulk ratio also affects strongly the CO hydrogenation activity (Fig. 7, inset top). It appears that the reducibility of the catalyst influences the CO hydrogenation activity comparing the H_2-TPR profiles recorded after the CO cycles (Fig. 7, inset middle): the lower the copper content in the catalyst the easier the reducibility (shift to lower temperature) and the higher the MeOH yield. Accordingly, the redox properties of the catalyst surface and so the interaction of Cu with ZnO seem to be important for CO hydrogenation, too.[50,51]

The uniqueness of the Cu-ZnO composition remains controversial. The interaction of ZnO with the adsorbed reactants of methanol synthesis (CO, CO_2, and H_2) was formerly studied by several authors.[52-54] In addition to the impact on the oxidation state of Cu by ZnO,[35,55] it is obvious that zinc oxide itself is involved in the reaction mechanism as an active site.[48,56-59] Otherwise the low activity of CuAl even at $R = 0$ could be not explained (Fig. 6). Topsøe *et al.* proposed a model of Cu-Zn alloy as active sites which are supposed to be formed *in situ* under strong reducing conditions (CO) accompanied by a migration of Zn to the catalyst surface.[18,60,61] Indeed, we could monitor such surface enrichment of Zn (Fig. 5a) and a shift of the zinc Auger signal at $R = 0$ (Fig. SI2) indicating a minor abundance of Zn^0. However, a clear proof for these sites was not found and their impact on CO_2-promoted MeOH synthesis remains therefore speculative.

Another theory involves the oxygen vacancies on ZnO as active sites.[59,62,63] The result of CO_2 inhibiting methanol production over $ZnO-Al_2O_3$ was interpreted to be the reason why a certain ratio R is needed for the reaction keeping the oxygen vacancies highly abundant through the reduction by CO. It emerges thereof that electron deficient zinc sites could have a significant impact on methanol synthesis. However, the inactivity of $ZnO-Al_2O_3$ in our experiments leads us to the conclusion that Zn might not participate directly in all reaction steps. Other authors concluded that the oxygen vacancies on ZnO influence the Cu/ZnO_x interface energy and therefore the morphology of the Cu nanoparticles.[19,41]

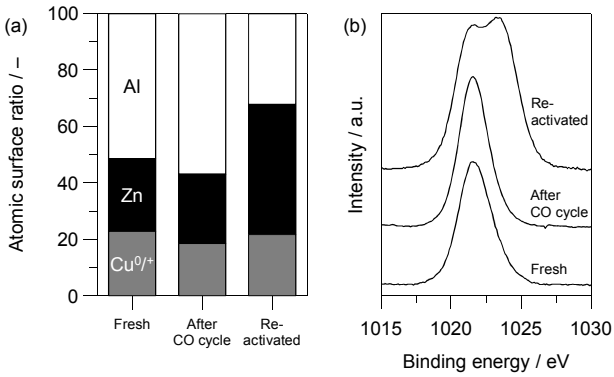

Fig. 9 (a) Surface composition and (b) Zn $2p_{3/2}$ spectra of CuZnAl fresh, after one CO cycle, and after re-activation and a subsequent CO cycle (*vide* Fig. 4a).

Consequently, this morphology alters dynamically according to the syngas composition. This structural feature seems to be unique for ZnO since other supports like SiO_2 do not exhibit such an interplay.

The type of interaction between Cu and ZnO will unambiguously determine the performance of the catalyst. This is affirmed by conducting the CO cycle over impregnated Al_2O_3 catalysts (Fig. 8): CO_2 promotion is only observed when the copper precursor is deposited on ZnO/Al_2O_3 (Cu@Zn). This catalyst offers easier reducible copper sites which indicates a better interaction of Cu and ZnO (*vide* H_2-TPR profiles in Fig. SI3) and is also responsible for the enhanced CO hydrogenation performance; in line with the correlation found for the co-precipitated CuZn catalysts (Fig. 7, inset top). The much higher dispersion of the Cu nanoparticles in Cu@Zn explains the higher CO_2 hydrogenation activity (*vide* $R = 100_{(1)}$ in Fig. 8). The combination of both structural properties seems to be the pre-requisite for CO_2 promotion. The flattened shape of the cycle might be a consequence of the low copper content in the impregnated catalysts, and therefore they are less affected by the detrimental hydroxyl coverage at higher R.

Finally, we have found that Al_2O_3 acts as important structural promoter in methanol synthesis catalysts. It is only a minor

View Article Online
DOI: 10.1039/C3CY00573A

compound in the bulk composition; however, it is highly abundant on the catalyst surface (Fig. 9a). Alumina enhances the dispersion of Cu nanoparticles and stabilises them (Fig. 6, inset). It has also impact on the Cu-ZnO interactions which explains its importance in terms of CO_2 promotion: the amount of Zn on the surface is doubled at the expense of Al after the CO cycle over re-activated CuZnAl (Fig. 9a). This increase of ZnO fraction can be assigned to isolated islands evidenced by the second peak appearing at ~1024 eV binding energy in the Zn $2p_{3/2}$ spectrum (Fig. 9b).

The strong influence of Al_2O_3 on the Cu-ZnO interaction is further evidenced by the CO cycles over the impregnated catalysts (Fig. 8): the hysteresis loop is not closing. The excess of Al_2O_3 appears to influence the reducibility of the catalysts and thus the CO hydrogenation performance which could be caused by the fixation of particular structural arrangements of Cu and ZnO formed along the cycle. These results substantiate former discussions on the importance of the microstructure of Cu-based catalysts and the influence by Al_2O_3 on it.[64,65] It is finally the interplay of cascading stabilisation of differently active Cu species by the metal oxides, ZnO and Al_2O_3, and the ability of dynamic alteration of the active sites which determines the catalyst behaviour in CO_2-promoted methanol synthesis.

4. Conclusions

The dynamic nature of Cu-ZnO-Al_2O_3 catalysts in CO_2-promoted methanol synthesis could be clearly unveiled by means of consecutively altering the CO_2 concentration in the syngas feed over various catalyst compositions and samples prepared *via* different routes. Kinetic descriptions therefore need to take into account that the active sites are not necessarily the same for all syngas compositions and that these sites are changed depending on the catalyst history. Consequently, turn over frequencies solely based on the copper surface area do not appear to be sufficient for investigating this reaction. Novel key findings of this study and revisited controversial results from literature are summarised in the following:

(1) The performance of Cu-based catalysts in CO_2-promoted methanol synthesis depends on the syngas composition and the history of the catalyst resulting in a hysteresis phenomenon. This behaviour is less affected by transient changes since a quasi-equilibrated catalyst exhibited a similar performance.

(2) It turned out unambiguously that the surface area of copper is not the key parameter for understanding the promotional effect since CO hydrogenation does not show a dependence on the copper surface area whereas CO_2 hydrogenation does. In line with reported results by several authors, the microstructure of the catalyst needs to be considered thoroughly.

(3) The promotional effect by CO_2 is coupled to the WGS activity. The deactivation at higher concentrations of CO_2 is thus a result of the excessive presence of surface hydroxyl species accompanied by the decrease in Cu dispersion which is detrimental for CO_2 hydrogenation.

(4) A strong evidence was found that the interaction of copper and zinc oxide dictates essentially the CO_2 promotion substantiating results formerly reported.

(5) The observed hysteresis appears to be the consequence of two effects: (i) the continuous decrease of Cu dispersion and (ii) the enhanced fixation of copper in its monovalent oxidation state. Both are disadvantageous for CO_2 hydrogenation (the first aspect is also detrimental for WGS).

Acknowledgements

We thank Total Research & Technology Feluy for permission to publish these results. Thomas Soltermann is acknowledged for his contribution to the preparation of the catalysts.

References

1 J. B. Hansen and P. E. H. Nielsen, in *Handbook of Heterogeneous Catalysis*, eds. G. Ertl, H. Knözinger, F. Schüth and J. Weitkamp, Wiley-VCH Verlag GmbH & Co. KGaA, Weinheim, 2nd edn., 2008, vol. 6, 2920.
2 K. Klier, *Adv. Catal.*, 1982, **31**, 243.
3 G. A. Olah, *Angew. Chem., Int. Ed.*, 2005, **44**, 2636.
4 B. Tidona, C. Koppold, A. Bansode, A. Urakawa and P. R. von Rohr, *J. Supercrit. Fluids*, 2013, **78**, 70.
5 Reaction enthalpies have been calculated using equation of state for ideal gases by software HSC Chemistry 7.1.
6 S. Lee, *Methanol Synthesis Technology*, CRC Press, Boca Raton, 1990.
7 Y. L. Zhang, Q. Sun, J. F. Deng, D. Wu and S. Y. Chen, *Appl. Catal., A*, 1997, **158**, 105.
8 K. Klier, V. Chatikavanij, R. G. Herman and G. W. Simmons, *J. Catal.*, 1982, **74**, 343.
9 K. G. Chanchlani, R. R. Hudgins and P. L. Silveston, *J. Catal.*, 1992, **136**, 59.
10 J. A. Brown Bourzutschky, N. Homs and A. T. Bell, *J. Catal.*, 1990, **124**, 73.
11 G. Liu, D. Willcox, M. Garland and H. H. Kung, *J. Catal.*, 1985, **96**, 251.
12 C. J. Schack, M. A. McNeil and R. G. Rinker, *Appl. Catal.*, 1989, **50**, 247.
13 J. S. Lee, K. H. Lee, S. Y. Lee and Y. G. Kim, *J. Catal.*, 1993, **144**, 414.
14 G. Prieto, J. Zečević, H. Friedrich, K. P. de Jong and P. E. de Jongh, *Nature Mater.*, 2013, **12**, 34.
15 J. C. J. Bart and R. P. A. Sneeden, *Catal. Today*, 1987, **2**, 1.
16 G. C. Chinchen, P. J. Denny, J. R. Jennings, M. S. Spencer and K. C. Waugh, *Appl. Catal.*, 1988, **36**, 1.
17 K. C. Waugh, *Catal. Lett.*, 2012, **142**, 1153.
18 J. D. Grunwaldt, A. M. Molenbroek, N.-Y. Topsøe, H. Topsøe and B. S. Clausen, *J. Catal.*, 2000, **194**, 452.
19 P. L. Hansen, J. B. Wagner, S. Helveg, J. R. Rostrup-Nielsen, B. S. Clausen and H. Topsøe, *Science*, 2002, **295**, 2053.
20 H. Wilmer and O. Hinrichsen, *Catal. Lett.*, 2002, **82**, 117.
21 H. Topsøe, C. V. Ovesen, B. S. Clausen, N.-Y. Topsøe, P. E. H. Nielsen, E. Törnqvist and J. K. Nørskov, in *Dynamics of Surfaces and Reaction Kinetics in Heterogeneous Catalysis*, eds. G. F. Froment and K. C. Waugh, Elsevier Science Bv, Amsterdam, 1997, vol. 109, 121.

View Article Online
DOI: 10.1039/C3CY00573A

22 M. Behrens, F. Studt, I. Kasatkin, S. Kühl, M. Hävecker, F. Abild-Pedersen, S. Zander, F. Girgsdies, P. Kurr, B.-L. Kniep, M. Tovar, R. Fischer, J. K. Nørskov and R. Schlögl, *Science*, 2012, **336**, 893.

23 Y. Yang, J. Evans, J. A. Rodriguez, M. G. White and P. Liu, *Phys. Chem. Chem. Phys.*, 2010, **12**, 9909.

24 C. Kuechen and U. Hoffmann, *Chem. Eng. Sci.*, 1993, **48**, 3767.

25 H.-W. Lim, M.-J. Park, S.-H. Kang, H.-J. Chae, J. W. Bae and K.-W. Jun, *Ind. Eng. Chem. Res.*, 2009, **48**, 10448.

26 K. L. Ng, D. Chadwick and B. A. Toseland, *Chem. Eng. Sci.*, 1999, **54**, 3587.

27 K. M. Vanden Bussche and G. F. Froment, *J. Catal.*, 1996, **161**, 1.

28 G. C. Chinchen, C. M. Hay, H. D. Vandervell and K. C. Waugh, *J. Catal.*, 1987, **103**, 79.

29 W. L. Dai, Q. Sun, J. F. Deng, D. Wu and Y. H. Sun, *Appl. Surf. Sci.*, 2001, **177**, 172.

30 P. Villa, P. Forzatti, G. Buzzi-Ferraris, G. Garone and I. Pasquon, *Ind. Eng. Chem. Process Des. Dev.*, 1985, **24**, 12.

31 G. Liu, D. Willcox, M. Garland and H. H. Kung, *J. Catal.*, 1984, **90**, 139.

32 F. Arena, K. Barbera, G. Italiano, G. Bonura, L. Spadaro and F. Frusteri, *J. Catal.*, 2007, **249**, 185.

33 S. Kaluza, M. Behrens, N. Schiefenhövel, B. Kniep, R. Fischer, R. Schlögl and M. Muhler, *ChemCatChem*, 2011, **3**, 189.

34 A. Karelovic, A. Bargibant, C. Fernández and P. Ruiz, *Catal. Today*, 2012, **197**, 109.

35 J. Nakamura, T. Uchijima, Y. Kanai and T. Fujitani, *Catal. Today*, 1996, **28**, 223.

36 Y. Yang, C. A. Mims, D. H. Mei, C. H. F. Peden and C. T. Campbell, *J. Catal.*, 2013, **298**, 10.

37 M. Sahibzada, I. S. Metcalfe and D. Chadwick, *J. Catal.*, 1998, **174**, 111.

38 M. Saito, T. Fujitani, M. Takeuchi and T. Watanabe, *Appl. Catal., A*, 1996, **138**, 311.

39 M. Peter, M. B. Fichtl, H. Ruland, S. Kaluza, M. Muhler and O. Hinrichsen, *Chem. Eng. J.*, 2012, **203**, 480.

40 M. J. L. Ginés, N. Amadeo, M. Laborde and C. R. Apesteguía, *Appl. Catal., A*, 1995, **131**, 283.

41 C. V. Ovesen, B. S. Clausen, J. Schiotz, P. Stoltze, H. Topsøe and J. K. Nørskov, *J. Catal.*, 1997, **168**, 133.

42 M. Peter, J. Fendt, S. Pleintinger and O. Hinrichsen, *Catal. Sci. Technol.*, 2012.

43 P. C. K. Vesborg, I. Chorkendorff, I. Knudsen, O. Balmes, J. Nerlov, A. M. Molenbroek, B. S. Clausen and S. Helveg, *J. Catal.*, 2009, **262**, 65.

44 G. U. Kulkarni and C. N. R. Rao, *Top. Catal.*, 2003, **22**, 183.

45 G. R. Apai, J. R. Monnier and M. J. Hanrahan, *J. Chem. Soc., Chem. Commun.*, 1984, 212.

46 J. R. Monnier, G. Apai and M. J. Hanrahan, *J. Catal.*, 1984, **88**, 523.

47 T. Fujitani and J. Nakamura, *Catal. Lett.*, 1998, **56**, 119.

48 R. G. Herman, K. Klier, G. W. Simmons, B. P. Finn, J. B. Bulko and T. P. Kobylinski, *J. Catal.*, 1979, **56**, 407.

49 G. C. Chinchen, K. Mansfield and M. S. Spencer, *Chemtech*, 1990, **20**, 692.

50 R. Burch and R. J. Chappell, *Appl. Catal.*, 1988, **45**, 131.

51 M. Amara, M. Bettahar and D. Olivier, *Appl. Catal.*, 1989, **51**, 141.

52 R. Naumann d'Alnoncourt, X. Xia, J. Strunk, E. Löffler, O. Hinrichsen and M. Muhler, *Phys. Chem. Chem. Phys.*, 2006, **8**, 1525.

53 D. L. Roberts and G. L. Griffin, *Appl. Surf. Sci.*, 1984, **19**, 298.

54 C. Wöll, *Prog. Surf. Sci.*, 2007, **82**, 55.

55 J. Skrzypek, M. Lachowska, M. Grzesik, J. Sloczynski and P. Nowak, *Chem. Eng. J. Biochem. Eng. J.*, 1995, **58**, 101.

56 V. E. Ostrovskii, *Catal. Today*, 2002, **77**, 141.

57 M. S. Spencer, *Top. Catal.*, 1999, **8**, 259.

58 X. M. Liu, G. Q. Lu, Z. F. Yan and J. Beltramini, *Ind. Eng. Chem. Res.*, 2003, **42**, 6518.

59 S. Polarz, J. Strunk, V. Ischenko, M. W. E. van den Berg, O. Hinrichsen, M. Muhler and M. Driess, *Angew. Chem., Int. Ed.*, 2006, **45**, 2965.

60 N.-Y. Topsøe and H. Topsøe, *J. Mol. Catal. A: Chem.*, 1999, **141**, 95.

61 N.-Y. Topsøe and H. Topsøe, *Top. Catal.*, 1999, **8**, 267.

62 M. Kurtz, J. Strunk, O. Hinrichsen, M. Muhler, K. Fink, B. Meyer and C. Wöll, *Angew. Chem., Int. Ed.*, 2005, **44**, 2790.

63 G. Rossmüller, V. Kleinschmidt, J. Kossmann and C. Hättig, *J. Phys. Chem. C*, 2009, **113**, 1418.

64 I. Kasatkin, P. Kurr, B. Kniep, A. Trunschke and R. Schlögl, *Angew. Chem., Int. Ed.*, 2007, **46**, 7324.

65 M. Kurtz, H. Wilmer, T. Genger, O. Hinrichsen and M. Muhler, *Catal. Lett.*, 2003, **86**, 77.

View Article Online
DOI: 10.1039/C3CY00573A

Table of content

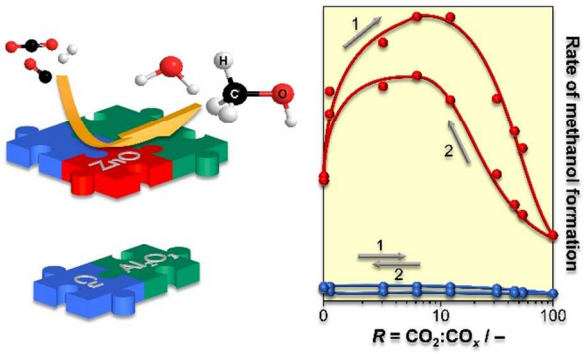

The CO_2-promoted methanol synthesis over binary and ternary Cu-based catalysts has been assessed by using cyclic tests in $CO:H_2:CO_2:H_2O$ mixtures.